NO$_3$ chemistry of wildfire emissions: a kinetic study of the gas-phase reactions of furans with the NO$_3$ radical

Mike J. Newland, Yangang Ren, Max R. McGillen, Lisa Michelat, Véronique Daële, Abdelwahid Mellouki

ICARE-CNRS, 1 C Av. de la Recherche Scientifique, 45071 Orléans Cedex 2, France

Correspondence to: Mike J. Newland (mike.newland@cnrs-orleans.fr; mellouki@cnrs-orleans.fr)

Abstract. Furans are emitted to the atmosphere during biomass burning from the pyrolysis of cellulose. They are one of the major contributing VOC classes to OH and NO$_3$ reactivity in biomass burning plumes. The major removal process of furans from the atmosphere at night is reaction with the nitrate radical, NO$_3$. Here we report a series of relative rate experiments in the 7300 L indoor simulation chamber at CNRS-ICARE, Orléans, using a number of different reference compounds to determine NO$_3$ reaction rate coefficients for four furans, two furanones, and pyrrole. In the case of the two furanones, this is the first time that NO$_3$ rate coefficients have been reported. The recommended values (cm^3 molecule^{-1} s^{-1}) are: furan $(1.49\pm0.23)\times10^{-12}$, 2-methylfuran $(2.26\pm0.52)\times10^{-11}$, 2,5-dimethylfuran $(1.02\pm0.31)\times10^{-10}$, furfural (furan-2-aldehyde) $(9.07\pm2.3)\times10^{-14}$, α-angelicalactone (5-methyl-2(3H)-furanone) $(3.01\pm0.45)\times10^{-12}$, γ-crotonolactone (2(5H)-furanone) $<1.4\times10^{-16}$, and pyrrole $(6.94\pm1.9)\times10^{-11}$. The furfural + NO$_3$ reaction rate coefficient is found to be an order of magnitude smaller than previously reported. These experiments show that for furan, alkyl substituted furans, α-angelicalactone, and pyrrole, reaction with NO$_3$ will be the dominant removal process at night, and may also contribute during the day. For γ-crotonolactone, reaction with NO$_3$ is not an important atmospheric sink.

1 Introduction

Furans are five membered aromatic cyclic ethers. Furans (and pyrroles – where N replaces O as the heteroatom) are generated during the pyrolysis of cellulose and are a major component of emissions from wildfire burning (Hatch et al., 2015, 2017; Koss et al., 2018; Coggon et al., 2019; Andreae et al., 2019). Such emissions are likely to increase in the future with the spatial extent, number, and severity, of wildfires globally having increased markedly in recent decades (Jolly et al., 2015; Harvey, 2016) and predicted to continue to do so as the climate warms (Krikken et al., 2019; Lohmander, 2020). Furans have also been measured in emissions from residential logwood burning (Hartikainen et al., 2018), and burning of a wide variety of solid-fuels used for domestic heating and cooking (Stewart et al., 2021a). Furans have been shown to account for a significant proportion of the total NO$_3$ (Decker et al., 2019) and OH (Koss et al., 2018; Coggon et al., 2019; Stewart et al., 2021b) reactivity of emissions from burning of typical wildfire and domestic fuels.

Alkyl substituted furans have also been suggested as promising biofuels as they can be derived from lignocellulosic biomass (Roman-Leshkov et al., 2007; Binder et al., 2009; Wang et al., 2014). This would likely lead to fugitive emissions of these compounds during distribution, as well as emissions of unburned and partially oxidised products from vehicle exhaust. The oxidation of certain furan compounds has been shown to have large secondary organic aerosol yields (Hatch et al., 2017; Hartikainen et al., 2018; Joo et al., 2019, Ahern et al., 2019; Akherati et al., 2020), which could adversely impact air quality.

Oxidation of furans in the atmosphere has been shown to produce 2-furanones (mono-unsaturated five-membered cyclic esters) both via OH (notably hydroxy-furan-2-ones, Aschmann et al., 2014) and NO$_3$ (Berndt et al., 1997) reactions. 2-Furanones are

38 also produced from the OH oxidation of six-membered aromatic compounds (Smith et al., 1998, 1999; Hamilton et al., 2005;
39 Bloss et al., 2005; Wyche et al., 2009; Huang et al., 2015). In both cases, the initial product is thought to be an unsaturated
40 dicarbonyl, with production of the 2-furanone formed via photoisomerisation of the dicarbonyl to a ketene-enol (Newland et al.,
41 2019), followed by ring closure of this molecule. In the case of aromatics, the ketene-enol can also be formed directly via
42 decomposition of the bicyclic peroxy radical intermediate (Wang et al., 2020).

43 Furan type compounds are removed from the atmosphere by reaction with the major oxidants OH, NO_3 and O_3. There have been
44 a number of studies on the rates of reaction of furan type compounds with the dominant daytime oxidant, OH (Lee and Tang,
45 1982; Atkinson et al., 1983; Wine and Thompson, 1984; Bierbach et al., 1992, 1994, 1995; Aschmann et al., 2011; Ausmeel et
46 al., 2017; Whelan et al., 2020). However, there have been fewer studies on the rates of reaction of furan type compounds with
47 the major night-time oxidant, NO_3 (Atkinson et al., 1985; Kind et al., 1996; Cabañas et al., 2004; Colmenar et al., 2012).

48 The nitrate radical, NO_3, is produced in the atmosphere predominantly through the reaction of NO_2 with O_3, and exists in
49 equilibrium with N_2O_5. It has long been known to be an important night-time oxidant (Levy, 1972; Winer et al., 1984). While it
50 is also produced during the daytime, it is rapidly converted back to NO_2 by reaction with NO and by photolysis. However, in
51 environments with low NO, either due to low NOx emissions, or suppression through high O_3 concentrations (e.g. Newland et
52 al., 2021), NO_3 oxidation has been observed to be significant during the day (Hamilton et al., 2021).

53 Here, we present results of a series of relative rate experiments for furan, 2-methylfuran, 2,5-dimethylfuran, furfural (furan-2-
54 aldehyde), α-angelicalactone (5-methyl-2(3H)-furanone), γ-crotonolactone (2(5H)-furanone), and pyrrole reaction with the NO_3
55 radical, performed in the 7300 L indoor simulation chamber at CNRS-ICARE, Orléans, France.

56 **2 Experimental**

57 **2.1   CSA-Chamber**

58

59 The CNRS-ICARE indoor chamber is a 7300 L indoor simulation chamber used for studying reaction kinetics and mechanisms
60 under atmospheric boundary layer conditions. Further details of the chamber setup and instrumentation are available elsewhere
61 (Zhou et al., 2017). Experiments were performed in the dark at atmospheric pressure (*ca.* 1000 mbar), with the chamber operated
62 at a slight overpressure to compensate for removal of air for sampling, and to prevent ingress of outside air to the chamber. The
63 chamber is in a climate controlled room and the temperature was maintained at 299±2 K.

64

65 **2.2   Experimental Approach**

66

67 Starting with the chamber filled with clean air, the VOCs of interest (*ca.* 3 ppmv) were added, followed by ~ 1 Torr of the inert
68 gas SF_6 to monitor the chamber dilution rate. The chamber was left for at least thirty minutes prior to the start of the experiment
69 to monitor the dilution rate and losses of the VOCs to the chamber walls. These losses, $(1-8)\times10^{-6}\,s^{-1}$, were always smaller than
70 dilution $(\sim1.2\times10^{-5}\,s^{-1})$. The reaction was then initiated by continuously introducing an N_2O_5 sample, held in a trap at ~ 235 K
71 with air flow of $(2.5-5)$ L/min through it, for the duration of the experiment. The chamber was monitored until most of the
72 VOC of interest was consumed, with experiments generally taking $0.5-2$ hours. The experiments were performed under dry
73 conditions (RH ≤ 1.5 %).

74 VOC abundance was determined by *in-situ* Fourier Transform Infrared (FTIR) Spectroscopy using a Nicolet 5700 coupled to a

75 White-type multipass cell with a pathlength of 143 m. Each scan was comprised of either 30 or 60 co-additions, taking a total of

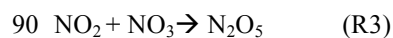76 2 or 4 minutes respectively, depending on the expected rate of loss of the VOCs, with a spectral resolution of 0.25 cm^{-1}.

77

2.3   Materials

79

80 The VOCs of interest: furan (>99%, Sigma-Aldrich), 2-methylfuran (>98%, TCI), 2,5-dimethylfuran (>98%, TCI), pyrrole

81 (>99%, TCI), α-angelicalactone (>98%, TCI), furfural (>98%, TCI), and γ-crotonolactone (>93%, TCI); and reference

82 compounds: α-terpinene (90%, Sigma-Aldrich), 2,3-dimethyl-but-2-ene (98%, Sigma-Aldrich), 2-carene (97%, Sigma-Aldrich),

83 camphene (95%, Sigma-Aldrich), α-pinene (98%, Sigma-Aldrich), cyclohexene (≥99%, Sigma-Aldrich), 3-methyl-3-buten-1-ol

84 (97%, Sigma-Aldrich), and cyclohexane (99.5%, Sigma-Aldrich), were used as supplied without further purification.

85 N_2O_5 was synthesised by reacting NO_2 with excess O_3. First, NO and O_3 were mixed to generate NO_2 (Reaction R1). This NO_2 /

86 O_3 mixture was then flushed into a bulb in which NO_3 and subsequently N_2O_5 were generated through Reactions R2-R3.

87

88 $NO + O_3 \rightarrow NO_2$ (R1)

89 $NO_2 + O_3 \rightarrow NO_3$ (R2)

90 $NO_2 + NO_3 \rightarrow N_2O_5$ (R3)

91

92 N_2O_5 crystals were then collected in a cold trap at 190K. The N_2O_5 sample was purified by trap to trap distillation under a flow

93 of O_2 / O_3. The final sample was stored at 190 K and used within a week.

94

2.4   Analysis

96

97 VOC concentrations were monitored by FTIR. The furans generally have a number of major absorption bands in the infrared.

98 The main bands used for analysis are shown in Table 1 (bold), as well as other characteristic bands for each compound. Reference

99 spectra of the major bands for each compound taken in the chamber at a resolution of 0.25 cm^{-1} are provided in the Supplement

100 (Figures S8-S14). The ANIR curve fitting software (Ródenas, 2018), which implements a least squares fitting algorithm was

101 used to generate time profiles for each compound based on their reference spectra. Profiles were checked by doing a number of

102 manual subtractions. Example time profiles from an experiment with α-angelicalactone and furan, with cyclohexene as the

103 reference compound, are shown in Figure 1. Further example plots are provided in the supplement (Figures S1-S7). All of the

104 concentration-time profiles are provided in .txt format at 10.5281/zenodo.5721518, and all the raw FTIR output is provided in

105 .csv format at 10.5281/zenodo.5721518. Relative rate plots for all of the experiments are shown in Figure 2.

106

107

108

109

110

111

112

113 **Table 1** Maxima of major absorption bands (of Q branches if present) for the compounds used in this study. Bands used
114 predominantly for analysis are shown in bold.

Compound	Main absorption bands / cm^{-1}
Furan	**995**, 744
2-Methylfuran	**792**, 726, 1151, 2965
2,5-Dimethylfuran	**777**, 2938, 2961
Furfural	**756**, 1720
Pyrrole	**724**, 1017, 3531, 718-722
α-angelicalactone	**731, 939**, 1100, 1834
γ-crotonolactone	**1098,** 805, 866, 1045, 1812, 2885, 2945
2,3-Dimethyl-2-butene	**2878, 2930, 3005**
2-Carene	**2874, 2928, 3009**
α-pinene	**2971, 2998, 3035,** 789, 2847, 2893, 2925, 2931
Camphene	**2967, 2972, 2986**, 882, 2881, 3075
Cyclohexene	**2934,** 744, 919, 1140, 2892, 2943, 3033, 3036
3-Methyl-3-buten-1-ol	**1065,** 896, 903, 2886, 2948, 2981, 3084
Cyclohexane	**2862, 2933**

115

116 Relative rate experiments were performed, whereby a compound (or two) with an unknown reaction rate coefficient (k_{VOC}) with
117 NO$_3$ was added to the chamber with a reference compound with a known NO$_3$ reaction rate coefficient (k_{ref}). A plot of the relative
118 loss of the compound against the reference compound following addition of NO$_3$ (via N$_2$O$_5$ decomposition), accounting for both
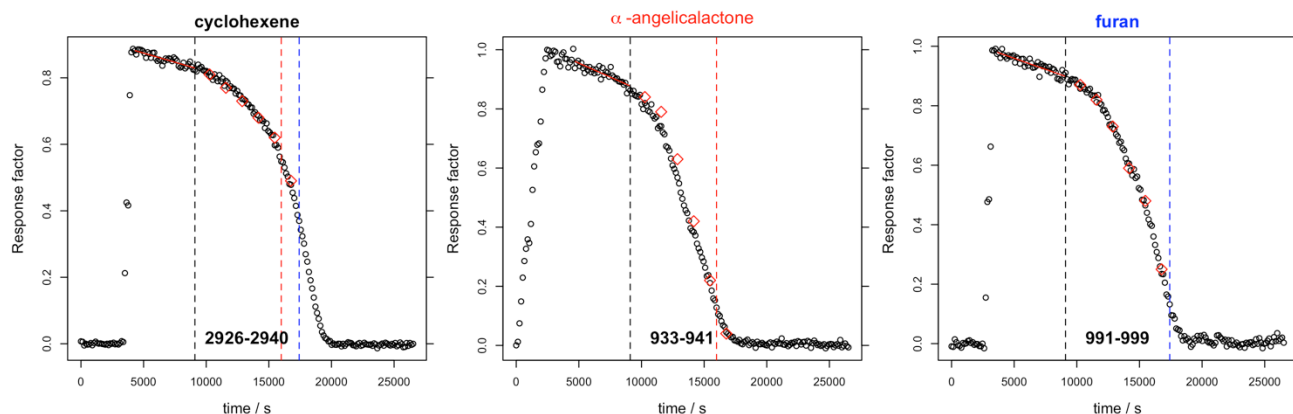119 chamber dilution and wall losses (k_d), gives a gradient of k_{VOC}/k_{ref} (Equation E1).

120

121
$$\ln \frac{([VOC]_0)}{([VOC]_t)} - k_d t = \frac{k_{VOC}}{k_{ref}} \ln \frac{[ref]_0}{[ref]_t} - k_d t \qquad \text{(E1)}$$

122

123 A number of reference compounds were used for each VOC, chosen so that the reference rate coefficient was roughly within a
124 factor of five of the expected unknown rate coefficient, and with an attempt to use different references that had both larger and
125 smaller NO$_3$ reaction rate coefficients than the VOC. Rate coefficients of the reference compounds (Table 2) are taken from the
126 Database for the Kinetics of the Gas-Phase Atmospheric Reactions of Organic Compounds v2.1.0 (McGillen et al., 2020),
127 available at data.eurochamp.org/data-access/kin/#/home.

128 N$_2$O$_5$ was not present at detectable levels (by FTIR) during most of the experiments. The only experiments in which N$_2$O$_5$
129 concentrations built up in the chamber, were those with the slowest reacting VOCs, i.e. furfural and γ-crotonolactone. NO$_2$
130 concentrations increased throughout all experiments, typically up to 2 – 3 ppmv. The NO$_2$ is initially produced from the
131 decomposition of N$_2$O$_5$, and later potentially by the loss of NO$_2$ from nitrated VOCs / nitrated radicals. HNO$_3$ concentrations
132 increased throughout the experiments, typically up to 3 – 4 ppmv. This could be either due to impurities in the N$_2$O$_5$ sample, or

133 from H abstraction reactions of NO_3. It is not thought that this level of HNO_3 will cause any interference in the rate coefficient
134 determinations.
135

136

137 **Figure 1** Concentration-time profiles from experiment with cyclohexene, α-angelicalactone and furan. Black circles are response
138 factors generated by the ANIR curve fitting program relative to the reference spectra. Red diamonds are obtained from manual
139 subtractions. Left black dashed vertical line is the beginning of the region used for the relative rate calculation, the red dashed
140 line is the end of the region used for the calculation of the α-angelicalactone relative rate, the blue line is the end of the region
141 used for the calculation of the furan relative rate. Bold values at the bottom are the absorption bands used for analysis.

142 **Table 2.** Reference compounds used. Recommended rate coefficients and uncertainties from McGillen et al. (2020).

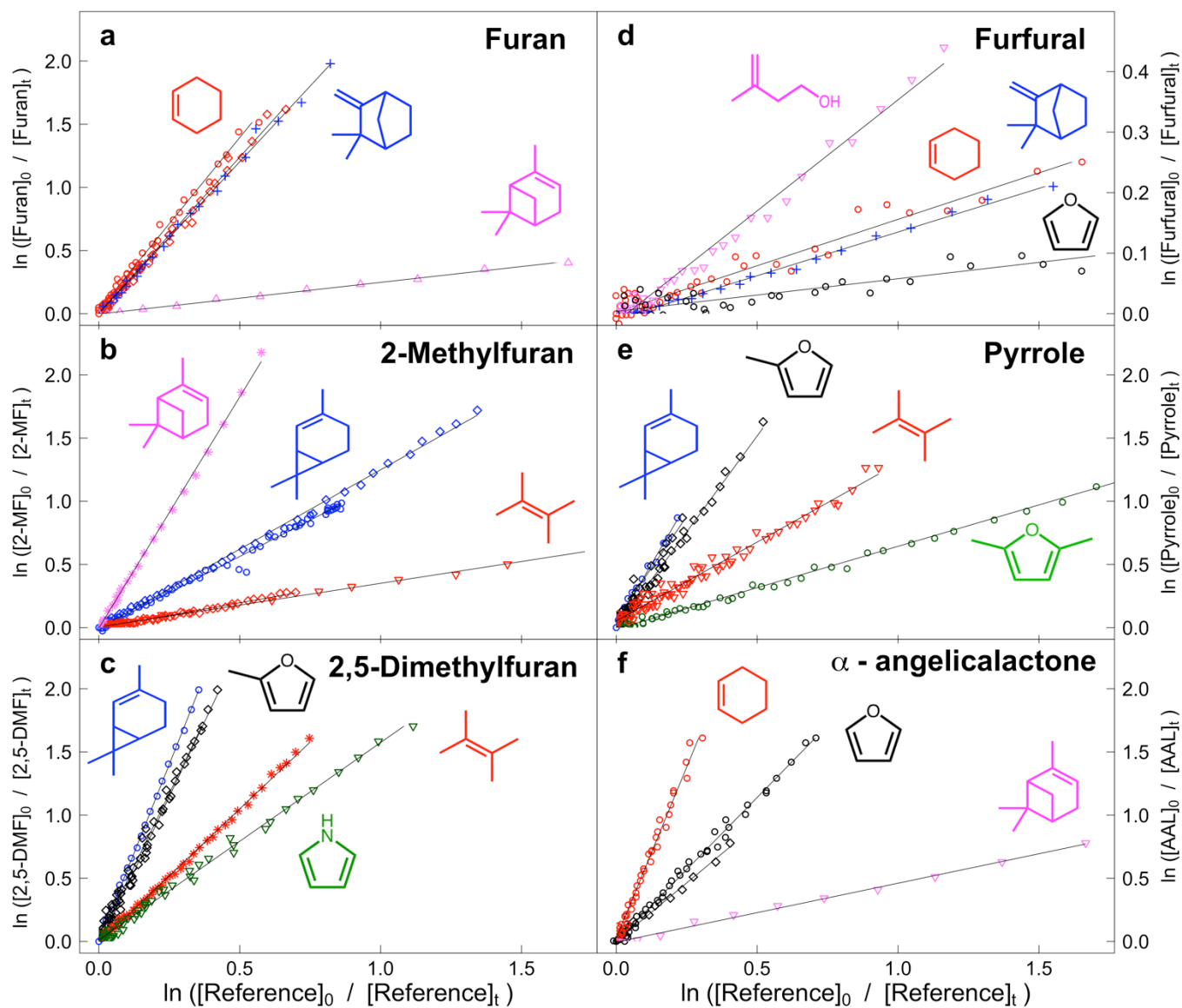| Compound	k / cm^3 $molecule^{-1}$ s^{-1}
2,3-dimethyl-2-butene	$(5.70\pm1.71)\times10^{-11}$
2-carene	$(2.0\pm0.3)\times10^{-11}$
α-pinene	$(6.20\pm1.55)\times10^{-12}$
camphene	$(6.60\pm1.65)\times10^{-13}$
cyclohexene	$(5.60\pm0.84)\times10^{-13}$
3-methyl-3-buten-1-ol	$(2.60\pm0.78)\times10^{-13}$
cyclohexane	$(1.35\pm0.20)\times10^{-16}$

143

144 It is noted that no OH scavenger was used in these experiments (as is the case for most, if not all, NO_3 previous relative rate
145 studies to the authors' knowledge). NO_3 reaction with alkenes tends to proceed by electrophilic addition to the double bond
146 followed by addition of O_2 to the resulting radical, leading to a nitrooxy peroxy radical (β-ONO_2-RO_2) (Barnes et al., 1989;
147 Hjorth et al., 1990). It has recently been shown (Novelli et al., 2021) that there is the possibility of OH formation through the
148 reactions of β-ONO_2-RO_2 with HO_2. HO_2 could be generated in these experiments from the abstraction of an H atom by O_2 from
149 a β-ONO_2-RO radical with available H atoms. The initial NO_3 reaction with furans is not thought to form β-ONO_2-RO_2 radicals,
150 with NO_3 addition to the C2 carbon followed by O_2 addition to the C_5 carbon (Berndt et al., 1997), analogous to the OH addition
151 reaction (Bierbach et al., 1995; Mousavipour et al., 2009; Yuan et al., 2017; Whelan et al., 2020). However, some of the reference
152 compounds used in the experiments will form such radicals. For example, the reaction of HO_2 with the β-ONO_2-RO_2 radicals
153 formed from α-pinene + NO_3 has been reported to have an OH yield of up to 70 % (Kurtén et al., 2017). An additional minor

154 source of HO_2 during the experiments will be H abstraction reactions by NO_3. These will produce RO_2 that can react to form RO

155 radicals which may yield HO_2 following abstraction of an H atom by O_2. However, the rate coefficient of H abstraction by NO_3

156 is generally expected to be negligible relative to that of the NO_3 addition pathway. A box model run was performed to test the

157 impact of this chemistry in this study. The α-pinene scheme from the MCMv3.3.1 (Jenkin et al., 1997; mcm.york.ac.uk) was

158 incorporated into the box model AtChem (Sommariva et al., 2020), and an OH yield of 0.5 was assigned to the reaction of HO_2

159 with the initial β-ONO_2-RO_2 radicals formed from the α-pinene+NO_3 reaction. The model was initiated with 2-methylfuran and

160 α-pinene concentrations of 3 ppmv, representative of the experiments performed here. NO_3 concentrations were constrained to

161 give a lifetime of ~ 1 hour for the VOCs, typical of the experiments. OH reaction was found to account for less than 1 % of the

162 removal of 2-methylfuran or α-pinene through the model run. Consequently, it can be assumed that OH chemistry is a negligible

163 interference in these experiments.

164 A further potential interference with the current experimental setup, is the reaction of NO_2 with the compounds used. Rate

165 coefficients have been measured for reaction of NO_2 with a number of unsaturated compounds. For conjugated dienes, these

166 values can be large enough (~10^{-18} cm^3 molecule^{-1} s^{-1}) to provide a significant loss under the experimental conditions employed

167 here (Atkinson et al., 1984; Bernard et al., 2013). NO_2 is formed during these experiments from the decomposition of N_2O_5, with

168 the NO_2 mixing ratio typically increasing up to roughly 3 ppmv through the experiment. Separate experiments were performed

169 to look at the potential reaction of NO_2 with furan, 2,5-dimethylfuran and pyrrole. For all three compounds, their loss in the

170 presence of NO_2 (allowing for dilution) was indistinguishable from zero, allowing an upper limit of < 2×10^{-20} cm^3 molecule^{-1} s^{-1}

171 to be placed on their $k(NO_2)$ rate coefficients.

172

Figure 2. Relative rate plots for: **a.** furan relative to cyclohexene (red), camphene (blue), and α-pinene (pink); **b.** 2-methylfuran relative to 2-carene (blue), 2,3-dimethyl-2-butene (red), and α-pinene (pink); **c.** 2,5-dimethylfuran relative to 2-carene (blue), 2,3-dimethyl-2-butene (red), 2-methylfuran (black), and pyrrole (green); **d.** furfural relative to camphene (blue), cyclohexene (red), furan (black), and 3-methyl-3-buten-1-ol (pink); **e.** pyrrole relative to 2-carene (blue), 2,3-dimethyl-2-butene (red), 2-methylfuran (black), and 2,5-dimethylfuran (green); **f.** α-angelicalactone relative to cyclohexene (red), furan (black), and α-pinene (pink). Different shapes are used for different experiments with the same reference compound.

3 Results and Discussion

The $k(NO_3)$ rate coefficients determined with each reference compound are given in Table 3 and Figure 3. A recommendation of an updated rate coefficient for α-terpinene+NO$_3$ is also given in Table 3. Overall recommended values for the rate coefficient for each compound are calculated by taking the mean (weighted by the reported uncertainty of the reference) of the rate coefficient derived from each experiment with each reference compound, including using the recommended values for the other

185 furans presented in Table 3. Uncertainties for the relative rates in Table S1 are assumed to be < 10 % and to be dominated by

186 statistical errors in fitting to the absorption bands. Uncertainties for the rate coefficients reported in Table 3 are dominated by

187 the assumed uncertainties in $k(NO_3)$ of the reference compounds. For most of the references, the uncertainties are 20 − 30 %,

188 taken from the recommendations of McGillen et al. (2020). For 2,3-dimethyl-2-butene, the recommended uncertainty in

189 McGillen et al. (2020) is 150 %, but based on the fact that the rate coefficients derived using 2,3-dimethyl-2-butene for 2-

190 methylfuran, 2,5-dimethylfuran and pyrrole agree very well with those using other references with much smaller uncertainties,

191 a conservative estimate of 30 % is used here. It is noted that for all compounds, the rate coefficients derived with different

192 references agree very well, to within 10%. The experimentally determined $k(NO_3)$ rate coefficients of the furans relative to each

193 other are in good agreement (to within 6%) with those calculated using the weighted means shown in Table 3 (Table S2). This

194 gives further confidence in the $k(NO_3)$ values used for the reference compounds.

195

196 The rate coefficient derived for furan, agrees well with the value previously reported by Atkinson et al. (1985) from a chamber

197 relative rate experiment. However, there is significant differences between the values reported here for furan, 2-methylfuran and

198 2,5-dimethylfuran, and those reported by Kind et al. (1996) from relative rate experiments in a flow reactor. While the value

199 reported for 2-methylfuran agrees within the uncertainties between the two studies, the values for furan and 2,5-dimethylfuran

200 are ~ 50 % and 100 % greater respectively. It is unclear what is behind this observed disparity; the good agreement between the

201 two studies for the 2-methylfuran rate coefficient suggests that there is not a systematic difference between the experimental

202 setups. For pyrrole, the rate coefficient determined here is about 50% faster than the value reported by Atkinson et al. (1985)

203 from a chamber relative rate experiment using N_2O_5 thermal decomposition. Cabañas et al. (2004) reported an upper limit of

204 $<1.8\times10^{-10}\,cm^3\,molecule^{-1}\,s^{-1}$ (298K) using an absolute technique of fast flow discharge.

205 For 2-furanaldehyde (furfural) + NO_3, the rate coefficient recommended here is an order of magnitude slower than the only

206 previously reported values (Colmenar et al., 2012), derived from small chamber relative rate experiments with 2-methyl-2-butene

207 and α-pinene as references. The rate coefficient from Colmenar et al. (2012) is very similar to the reported rate coefficient for

208 furan+NO_3. This is surprising, since the presence of a formyl group attached to a double bond is expected to be strongly

209 deactivating with respect to addition to that bond, due to the electron withdrawing mesomeric effect of the –C(O)H group

210 (Kerdouci et al., 2014). This has also been observed for other electrophilic addition reactions, such as those with OH and O_3

211 (Kwok and Atkinson, 1995; McGillen et al, 2011; Jenkin et al., 2020). And while there is the possibility of H abstraction from

212 the formyl group, which would increase the overall rate coefficient, such reactions are typically of the order of $10^{-14}\,cm^3s^{-1}$

213 (Kerdouci et al., 2014), and hence would not be expected to compensate for the reduction in the contribution to the overall rate

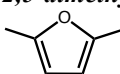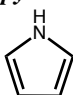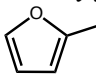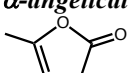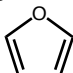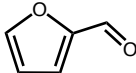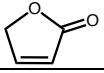214 coefficient of the addition reaction.

215 For 5-methyl-(3H)-furan-2-one (α-angelica lactone) + NO_3 this is the first reported rate coefficient. For (5H)-furan-2-one (γ-

216 crotonolactone), relative rate experiments with several reference compounds were attempted, with the slowest reacting of these

217 being cyclohexane (k_{NO3} = $1.4\times10^{-16}\,cm^3\,molecule^{-1}\,s^{-1}$). Roughly 10 % of the cyclohexane was removed in this experiment

218 (accounting for loss by dilution), with no appreciable loss of γ-crotonolactone. We can therefore deduce that k(γ-

219 crotonolactone+NO_3) << $1.4\times10^{-16}\,cm^3\,molecule^{-1}\,s^{-1}$. Again, this is the first time a NO_3 reaction rate coefficient has been

220 measured for this compound. A comparison of the two furanones shows that 5-methyl-(3H)-furan-2-one reacts more than four

221 orders of magnitude faster than (5H)-furan-2-one. This can be explained in part by the presence of a methyl group, which is seen

222 to increase the rate coefficient by roughly an order of magnitude from e.g. furan to 2-methylfuran to 2,5-dimethylfuran. Berndt

223 et al. (1997) derived an NO$_3$ reaction rate coefficient of 1.76×10^{-13} cm^3 molecule^{-1} s^{-1} for (3H)-furan-2-one. However, the majority

224 of the difference must be explained by the structure of the two compounds, namely the conjugated nature of the C=C and C=O

225 bonds in (5H)-furan-2-one. The carbonyl group removes electron density from the C=C bond greatly reducing the rate

226 coefficient. A similar relationship is seen for analogous acyclic compounds e.g. the NO$_3$ rate coefficient of the conjugated ester

227 methyl acrylate is almost two orders of magnitude greater than that of the non-conjugated isomer vinyl acetate.
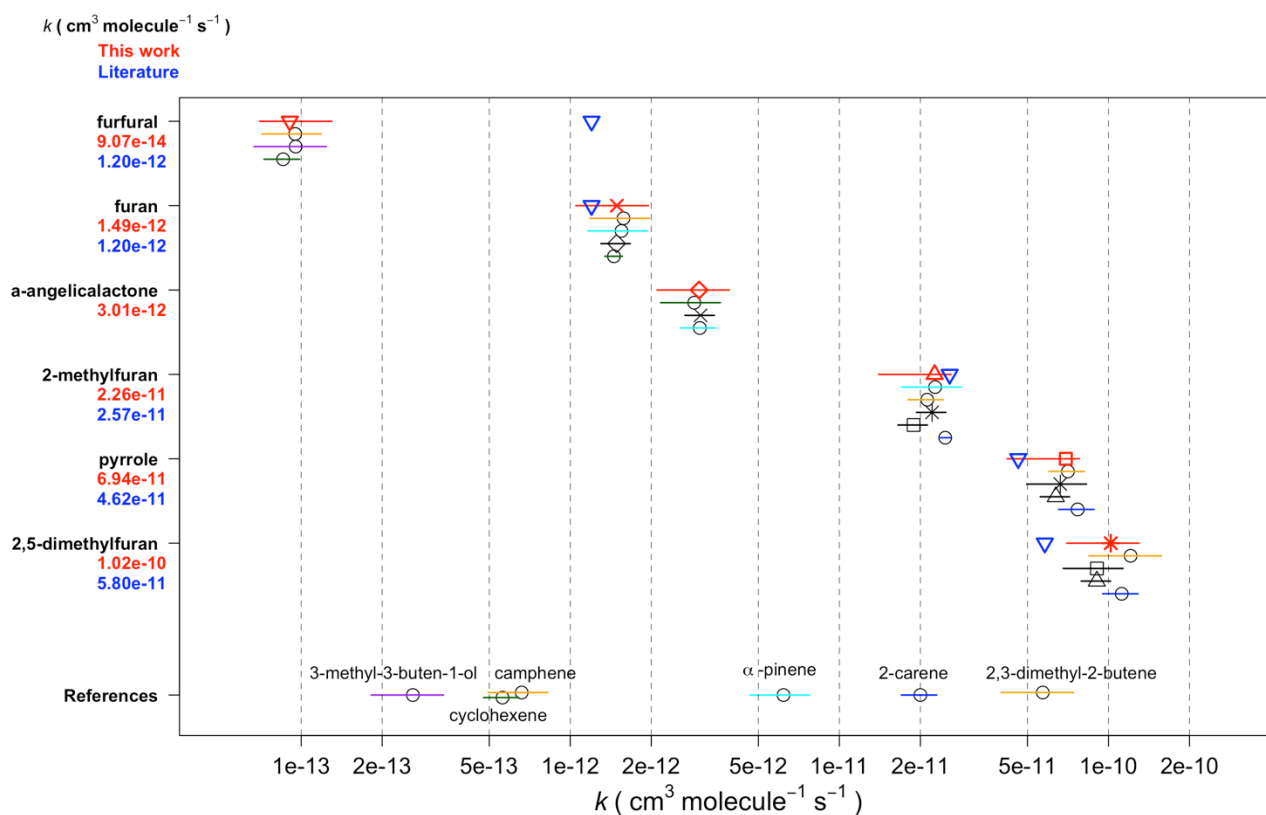
228

229

230 **Table 3.** NO$_3$ reaction rate coefficients derived for each experiment and recommended value based on the weighted mean.

Compound	Reference (repeats)	$k(NO_3)$ / cm^3 molecule^{-1} s^{-1}	Weighted mean $k(NO_3)$ / cm^3 molecule^{-1} s^{-1}
2,5-dimethylfuran	2-carene (1)	1.12×10^{-10}	**$1.02\pm0.31\times10^{-10}$**
	2,3-dimethyl-2-butene (1)	1.21×10^{-10}	
	pyrrole (1)	9.12×10^{-10}	
	2-methylfuran (2)	9.06×10^{-10}	
pyrrole	2-carene (1)	7.68×10^{-11}	**$6.94\pm1.9\times10^{-11}$**
	2,3-dimethyl-2-butene (2)	7.07×10^{-11}	
	2,5-dimethylfuran (1)	6.58×10^{-11}	
	2-methylfuran (2)	6.37×10^{-11}	
2-methylfuran	2-carene (3)	2.47×10^{-11}	**$2.26\pm0.52\times10^{-11}$**
	2,3-dimethyl-2-butene (2)	2.12×10^{-11}	
	α-pinene (1)	2.27×10^{-11}	
	pyrrole (2)	1.89×10^{-11}	
	2,5-dimethylfuran (2)	2.21×10^{-11}	
α-angelicalactone	α-pinene	2.89×10^{-12}	**$3.01\pm0.45\times10^{-12}$**
	cyclohexene	3.03×10^{-12}	
	furan (2)	3.05×10^{-12}	
furan	cyclohexene	1.45×10^{-12}	**$1.49\pm0.23\times10^{-12}$**
	α-pinene	1.55×10^{-12}	
	camphene	1.58×10^{-12}	
	α-angelicalactone (2)	1.49×10^{-12}	
furfural	cyclohexene (1)	8.57×10^{-14}	**$9.07\pm2.30\times10^{-14}$**
	3-methyl-3-buten-1-ol (1)	9.54×10^{-14}	
	camphene (1)	9.50×10^{-14}	
γ-crotonolactone	cyclohexane	$< 1.4\times10^{-16}$	**$< 1.4\times10^{-16}$**

231

232

Figure 3 The reaction rate coefficients derived for the six compounds in this work (excluding γ-crotonolactone). Red triangles (and red text, left axis) represent the weighted mean of all experiments in this work, blue inverted triangles (and blue text, left axis) are the recommended values from McGillen et al. (2020). Horizontal lines represent uncertainty in rate coefficient, colours (shapes if other furans) represent which reference was used.

Table 4. Recommended NO_3 rate coefficients from this work compared to those reported in the literature.

Compound	Rate coefficient / cm³ molecule⁻¹ s⁻¹	Reference	Technique	NO_3 source
2,5-dimethylfuran	**(1.02±0.31)×10⁻¹⁰**	**This work**		
	(5.78±0.34)×10⁻¹¹	Kind et al. (1996)	Flow reactor: relative (*trans*-2-butene)	N_2O_5
pyrrole	**(6.94±1.9)×10⁻¹¹**	**This work**		
	(4.6±1.1)×10⁻¹¹	Atkinson et al. (1985)	Chamber: relative (2-methyl-2-butene)	N_2O_5
	< 1×10⁻¹⁰	Cabañas et al. (2004)	Flow reactor: absolute (LIF detection of NO_3)	HNO_3+F
2-methylfuran	**(2.26±0.52)×10⁻¹¹**	**This work**		
	(2.57±0.17)×10⁻¹¹	Kind et al. (1996)	Flow reactor: relative (*trans*-2-butene)	N_2O_5
α-angelicalactone	**(3.01±0.45)×10⁻¹²**	**This work**		
furan	**(1.49±0.23)×10⁻¹²**	**This work**		
	(1.5±0.2)×10⁻¹² [b]	Atkinson et al. (1985)	Chamber: relative (*trans*-2-butene)	N_2O_5
	(0.998±0.062)×10⁻¹²	Kind et al. (1996)	Flow reactor: relative (*trans*-2-butene)	N_2O_5
	(1.36±0.8)×10⁻¹²	Cabañas et al. (2004)	Flow reactor: absolute (LIF detection of NO_3)	HNO_3+F

furfural	$(9.07\pm2.30)\times10^{-14}$	This work	
	$(1.17\pm0.15)\times10^{-12}$	Colmenar et al. (2012)	Small chamber: relative (2-methyl-2-butene) N_2O_5
	$(1.36\pm0.38)\times10^{-12}$	Colmenar et al. (2012)	Small chamber: relative (α-pinene) N_2O_5
γ-crotonolactone	$< 1.4\times10^{-16}$	This work	

241 [a] corrected for change to recommended rate for reference (2,3-dimethyl-2-butene); [b] corrected for change to recommended rate

242 for reference (trans-2-butene)

243

244 **4 Atmospheric implications**

245

246 The atmospheric lifetimes of the compounds, based on the rate coefficients reported herein, are given in Table 5. These assume

247 concentrations of OH = 5×10^6 molecules cm^{-3} (typical daily peak summertime concentrations $1.5\times10^6 - 1.5\times10^7$ molecules cm$^-$

248 ^{3} (Stone et al., 2012)), night-time NO$_3$ = 2×10^8 molecules cm^{-3} (typical night-time concentrations $1\times10^8 - >1\times10^9$ cm^{-3} (Brown

249 and Stutz (2012)) daytime NO$_3$ = 1×10^7 molecules cm^{-3} (limited daytime measurements suggest concentrations $\sim 0.5 - >1$ pptv

250 (2.5×10^7 molecules cm^{-3}) (Brown and Stutz (2012)), and O$_3$ = 40 ppbv (background O$_3$ concentration $\sim$ 40 ppb (Parrish et al.,

251 2014)). From these values it is clear that the alkyl substituted furans and pyrrole have very short lifetimes both during the day,

252 when the dominant daytime sink is likely to be reaction with OH, and at night, when the dominant sink will be reaction with

253 NO$_3$. O$_3$ may contribute somewhat to the removal of these compounds both during the day and night, particularly for 2,5-

254 dimethylfuran. As k(NO$_3$) approaches the same order of magnitude as k(OH), e.g. for 2-methylfuran, 2,5-dimethylfuran and

255 pyrrole, the NO$_3$ reaction is likely to be competitive with the OH reaction even during the day in low NOx environments, with

256 daytime NO$_3$ concentrations reported to be $\sim$ 1 ppt (2.5×10^7 molecules cm^{-3}) (Brown and Stutz, 2012). The relatively large rate

257 coefficient reported here for α-angelicalactone, suggests that NO$_3$ reaction will be an important sink for unsaturated non-

258 conjugated cyclic esters. On the other hand, the very small rate coefficient for the γ-crotonolactone +NO$_3$ reaction suggests that

259 this will not be an important atmospheric sink. γ-crotonolactone has also been shown to have a very slow reaction with O$_3$

260 (lifetime > 100 years, Ausmeel et al., 2017), whereas for reaction with OH, the lifetime is much shorter, and this will be the

261 predominant gas-phase sink for γ-crotonolactone . Such a slow NO$_3$ reaction might be expected to extend to all 2-furanones with

262 a conjugated structure, e.g. hydroxyfuranones – major products of OH oxidation of methyl substituted furans (Aschmann et al.,

263 2014), such that the nitrate reaction may be unimportant in the atmosphere for these structures. Although substitution at the

264 double bond is likely to increase the rate coefficient somewhat, as observed for OH and O$_3$ reactions with the methyl-substituted

265 form of γ-crotonolactone (Ausmeel et al., 2017).

266 One of the major sources of furan type compounds to the atmosphere is wildfires. Wildfire plumes can be regions of high NO$_3$

267 even during the day due to suppressed photolysis rates in optically thick plumes (Decker et al, 2021). NO$_3$ oxidation of furans

268 may be even more important in such plumes than in the background atmosphere. Such plumes can extend over hundreds of

269 kilometres and hence affect air quality on a local and regional scale (e.g. Andreae et al., 1988; Brocchi et al., 2018; Johnson et

270 al., 2021). Domestic wood burning is an increasing trend in northern European cities (Chafe et al., 2015). Burning will generally

271 be in the winter during which, with short daylight hours and peak daytime OH often an order of magnitude lower than during

272 the summer, the reaction with NO$_3$ is likely to be the dominant fate of furan type compounds in such emissions, contributing

273 significantly to organic aerosol in urban areas (Kodros et al., 2020).

274 Berndt et al. (1997) identified the major first generation products of furan+NO$_3$ to be the unsaturated dicarbonyl, butenedial, and
275 2(3H)-furanone, with the NO$_3$ recycled back to NO$_2$. However, Tapia et al. (2011), and Joo et al. (2019) found that the major
276 products of the 3-methylfuran+NO$_3$ reaction predominantly retain the NO$_3$ functionality. In this case, furan+NO$_3$ oxidation
277 chemistry may be a significant sink for NOx, sequestering it in nitrate species, which might release it far from source on further
278 gas-phase oxidation, or, due to their low volatility, be taken up into aerosol (Joo et al. 2019).
279

280 **Table 5.** Atmospheric gas-phase lifetimes of the compounds reported herein based on typical mid-day OH concentrations of
281 5×10^6 molecules cm^{-3}, night-time NO$_3$ concentrations of 2×10^8 molecules cm^{-3}, day-time NO$_3$ concentrations of 1×10^7 molecules
282 cm^{-3}, and background O$_3$ concentrations of 40 ppbv (1×10^{12} molecules cm^{-3}).

Compound	$\tau_{NO3 \text{ (night)}}$	$\tau_{NO3 \text{ (day)}}$	$\tau_{OH \text{ (day)}}$	τ_{O3}	$\tau_{total \text{ (day)}}$
2,5-dimethylfuran	0.82 min	16 min	26 min [a]	40 min [b]	8 min
2-methylfuran	3.7 min	74 min	48 min [a]	-	28 min
furan	56 min	19 hours	83 min [a]	116 hours [c]	77 min
pyrrole	1.2 min	24 min	28 min [d]	18 hours [d]	13 mins
furfural	15 hours	13 days	95 min [e]	-	94 min
α-angelicalactone	28 min	9.3 hours	48 min [f]	3.5 hours [g]	37 mins
γ-crotonolactone	> 1.1 year	> 22 years	14 hours [h]	173 years	14 hours

283 [a] Matsumoto (2011); [b] Dillon et al. (2012); [c] Atkinson et al. (1983); [d] Atkinson et al. (1984); [e] Bierbach et al. (1995); [f] Bierbach
284 et al. (1994); [g] estimated (Bierbach et al., 1994); [h] Ausmeel et al. (2017)

285 **5 Conclusions**

286 Rate coefficients are recommended for reaction of seven furan type VOCs with NO$_3$ at 298 K and 760 Torr, based on a series of
287 relative rate experiments. These new recommendations highlight the importance of NO$_3$ chemistry to the removal of furans, and
288 other similar VOCs, under atmospheric conditions. The measured rate coefficients suggest that for the three furans reported here,
289 as well as for pyrrole and α-angelicalactone, reaction with NO$_3$ is likely to be their dominant night-time sink. For the alkyl furans
290 and pyrrole, reaction with NO$_3$ may also be a significant sink during the daytime. This work also extends the existing database
291 of VOC+NO$_3$ reactions, providing valuable reference values for future work.
292

293

294 *Data availability.* Further example plots and experiment information are provided in the supplement. All of the response-time
295 profiles from the FTIR are provided in .txt format at 10.5281/zenodo.5724967, and all of the raw FTIR output is provided in .csv
296 format at 10.5281/zenodo.5721518.
297

298 *Author contributions.* MJN performed the experiments with the technical support of YR and MRM and performed the data
299 treatment and interpretation. MJN wrote the paper. All co-authors revised the content of the original manuscript and approved
300 the final version of the paper.
301

References

317 Ahern, A. T., Robinson, E. S., Tkacik, D. S., Saleh, R., Hatch, L. E., Barsanti, K. C., Stockwell, C. E., Yokelson, R. J., Presto,
318 A. A., Robinson, A. L., Sullivan, R. C., and Donahue, N. M.: Production of Secondary Organic Aerosol During Aging of Biomass
319 Burning Smoke From Fresh Fuels and Its Relationship to VOC Precursors, J. Geophys. Res.-Atmos., 124, 3583–3606, 2019.

320
321 Akherati, A., He, Y., Coggon, M. M., Koss, A. R., Hodshire, A. L., Sekimoto, K., Warneke, C., de Gouw, J., Yee, L., Seinfeld,
322 J. H., Onasch, T. B., Herndon, S. C., Knighton, W. B., Cappa, C. D., Kleeman, M. J., Lim, C. Y., Kroll, J. H., Pierce, J. R., and
323 Jathar, S. H.: Oxygenated Aromatic Compounds are Important Precursors of Secondary Organic Aerosol in Biomass Burning
324 Emissions, Environ. Sci. Technol., 54, 8568–8579, https://doi.org/10.1021/acs.est.0c01345, 2020.

325
326 Andreae, M. O., Browell, E. V., Garstang, M,. Gregory, G. L., Harriss, R. C., Hill, G. F., Jacob, D. J., Pereira, C., Sachse, G.
327 W., Setzer, A. W., Silva Dias, P. L., Talbot, R. W., Torres, A. L., and Wofsy, S. C.: Biomass-burning emissions and associated
328 haze layers over Amazonia, J. Geophys. Res.-Atmos, 93, 1509-1527, 1988.

329
330 Andreae, M. O.: Emission of trace gases and aerosols from biomass burning – an updated assessment, Atmos. Chem. Phys., 19,
331 8523–8546, https://doi.org/10.5194/acp-19-8523-2019, 2019.

332
333 Aschmann, S. M., Nishino, N., Arey J., and Atkinson, R.: Products of the OH radical-initiated reactions of furan, 2- and 3-
334 methylfuran, and 2,3- and 2,5-dimethylfuran in the presence of NO, J. Phys. Chem. A, 118, 457-466, 2014.

335
336 Atkinson, R., Aschmann, S. M., and Carter, W. P. L.: Kinetics of the reactions of O_3 and OH radicals with furan and thiophene
337 at 298 +/- 2 K, Int. J. Chem. Kinet., 15, 51-61, 1983.

338
339 Atkinson, R., Aschmann, S. M., Winer, A. M., and Carter, W. P. L.: Rate Constants for the Gas Phase Reactions of OH Radicals
340 and O_3 with Pyrrole at 295 +/- 1 K and Atmospheric Pressure, Atmos. Environ., 18, 2105-2107, 1984.

341
342 Atkinson, R., Aschmann, S. M., Winer, A. M., and Pitts, J. N.: Gas-phase reactions of NO_2 with alkenes and dialkenes, Int. J.
343 Chem. Kinet., 16, 697-706, 1984.

344

345 Atkinson, R., Aschmann, S. M., Winer, A. M., and Carter, W. P. L.: Rate Constants for the Gas Phase Reactions of NO_3 Radicals
346 with Furan, Thiophene and Pyrrole at 295 +/- 1 K and Atmospheric Pressure, Environ. Sci. Technol., 19, 87-90, 1985.
347
348 Ausmeel, S., Andersen, C., Nielsen, O. J., Østerstrøm, F. F., Johnson, M. S., and Nilsson, E. J. K.: Reactions of Three Lactones
349 with Cl, OD, and O_3: Atmospheric Impact and Trends in Furan Reactivity, J. Phys. Chem. A, 121, 4123-4131, 2017.
350
351 Barnes, I., Bastian, V., Becker, K. H., and Tong, Z.: Kinetics and products of the reactions of nitrate radical with monoalkenes,
352 dialkenes, and monoterpenes, J. Phys. Chem., 94, 2413–2419, 1990.
353
354 Bernard, F., Cazaunau, M., Mu, Y., Wang, X., Daële, V,. Chen, J., and Mellouki, A.: Reaction of NO_2 with conjugated alkenes,
355 J. Phys. Chem. A, 117, 14132-14140, 2013.
356
357 Berndt, T., Böge, O., Kind, I., and Rolle, W.: Reaction of NO_3 Radicals with 1,3-cyclohexadiene, α-terpinene, and α-
358 phellandrene, Ber. Bunsenges. Phys. Chem, 100, 462–469, 1996.
359
360 Berndt, T., Böge, O., and Rolle, W.: Products of the Gas-Phase Reactions of NO_3 Radicals with Furan and Tetramethylfuran,
361 Environ. Sci. Technol., 31, 1157–1162, 1997.
362
363 Bierbach, A., Barnes, I., Becker, K. H., and Wiesen, E.: Atmospheric Chemistry of Unsaturated Carbonyls: Butenedial, 4-Oxo-
364 2-pentenal, 3-Hexene-2,5-dione, Maleic Anhydride, 3H-Furan-2-one, and 5-Methyl-3H-furan-2-one, Environ. Sci. Technol., 28,
365 715-729, 1994.
366
367 Bierbach, A., Barnes, I., and Becker, K. H.: Product and kinetic study of the OH-initiated gas-phase oxidation of furan, 2-
368 methylfuran and furanaldehydes at ≈ 300 K, Atmos. Environ., 29, 2651–2660, 1995.
369
370 Binder, J. B., and Raines, R. T.: Simple Chemical Transformation of Lignocellulosic Biomass into Furans for Fuels and
371 Chemicals. J. Am. Chem. Soc., 131, 1979−1985, 2009.
372
373 Bloss, C., Wagner, V., Jenkin, M. E., Volkamer, R., Bloss, W. J., Lee, J. D., Heard, D. E., Wirtz, K., Martin-Reviejo, M., Rea,
374 G., Wenger, J. C., and Pilling, M. J.: Development of a detailed chemical mechanism (MCMv3.1) for the atmospheric oxidation
375 of aromatic hydrocarbons, Atmos. Chem. Phys., 5, 641–664, https://doi.org/10.5194/acp-5-641-2005, 2005.
376
377 Brocchi, V., Krysztofiak, G., Catoire, V., Guth, J., Marécal, V., Zbinden, R., El Amraoui, L., Dulac, F., and Ricaud, P.:
378 Intercontinental transport of biomass burning pollutants over the Mediterranean Basin during the summer 2014 ChArMEx-
379 GLAM airborne campaign, Atmos. Chem. Phys., 18, pp. 6887-6906, 2018.
380
381 Brown, S., and Stutz, J.: Nighttime radical observations and chemistry, Chem. Soc. Rev., 41, 6405-6447, 2012.
382
383 Cabañas, B., Baeza, M. T., Salgado, S., Martín, P., Taccone, R., and Martínez, E.: Oxidation of heterocycles in the atmosphere:
384 Kinetic study of their reactions with NO_3 radical, J. Phys. Chem. A, 108, 10818-10823, 2004.
385
386 Chafe, Z., Brauer, M., Héroux, M. –E., Klimont, Z., Lanki, T., Salonen, R. O., and Smith, K. R.: Residential heating with wood
387 and coal: health impacts and policy options in Europe and North America, WHO Regional Office for
388 Europe. https://apps.who.int/iris/handle/10665/153671, 2015.
389
390 Coggon, M. M., Lim, C. Y., Koss, A. R., Sekimoto, K., Yuan, B., Gilman, J. B., Hagan, D. H., Selimovic, V., Zarzana, K. J.,
391 Brown, S. S, M Roberts, J., Müller, M., Yokelson, R., Wisthaler, A., Krechmer, J. E., Jimenez, J. L., Cappa, C., Kroll, J. H., De
392 Gouw, J. and Warneke, C.: OH chemistry of non-methane organic gases (NMOGs) emitted from laboratory and ambient biomass
393 burning smoke: Evaluating the influence of furans and oxygenated aromatics on ozone and secondary NMOG formation, Atmos.
394 Chem. Phys., 19, 14875–14899, doi:10.5194/acp-19-14875-2019, 2019.

395

Colmenar, I., Cabañas, B., Martínez, E., Salgado, M. S., and Martín, P.: Atmospheric fate of a series of furanaldehydes by their NO_3 reactions, Atmos. Environ., 54, 177-184, 2012.

398

Decker, Z. C. J., Zarzana, K. J., Coggon, M., Min, K.-E., Pollack, I., Ryerson, T. B., Peischl, J., Edwards, P., Dubé, W. P., Markovic, M. Z., Roberts, J. M., Veres, P. R., Graus, M., Warneke, C., de Gouw, J., Hatch, L. E., Barsanti, K. C. and Brown, S. S.: Nighttime Chemical Transformation in Biomass Burning Plumes: A Box Model Analysis Initialized with Aircraft Observations, Environ. Sci. Technol., 53, 2529–2538, doi:10.1021/acs.est.8b05359, 2019.

403

Dillon, T. J., Tucceri, M. E., Dulitz, K., Horowitz, A., Vereecken, L., and Crowley, J.: Reaction of Hydroxyl Radicals with C4H5N (Pyrrole): Temperature and Pressure Dependent Rate Coefficients, J. Phys. Chem. A, 116, 6051-6058, 2012.

406

Fouqueau, A., Cirtog, M., Cazaunau, M., Pangui, E., Doussin J. -F., and Picquet-Varrault, B.: A comparative and experimental study of the reactivity with nitrate radical of two terpenes: α-terpinene and γ-terpinene, Atmos. Chem. Phys., 20, 15167-15189, 2020.

410

Harvey B. J.: Human-caused climate change is now a key driver of forest fire activity in the western United States, Proc. Natl. Acad. Sci., 113, 11649-11650, 2016.

413

Hartikainen, A., Yli-Pirilä, P., Tiitta, P., Leskinen, A., Kortelainen, M., Orasche, J., Schnelle-Kreis, J., Lehtinen, K., Zimmermann, R., Jokiniemi, J., and Sippula, O.: Volatile Organic Compounds from Logwood Combustion: Emissions and Transformation under Dark and Photochemical Aging Conditions in a Smog Chamber, Environ. Sci. Technol., 52, 4979-4988, 2018.

418

Hatch, L. E., Luo, W., Pankow, J. F., Yokelson, R. J., Stockwell, C. E., and Barsanti, K. C.: Identification and quantification of gaseous organic compounds emitted from biomass burning using two-dimensional gas chromatography–time-of-flight mass spectrometry, Atmos. Chem. Phys., 15, 1865–1899, https://doi.org/10.5194/acp-15-1865-2015, 2015.

422

Hatch, L. E., Yokelson, R. J., Stockwell, C. E., Veres, P. R., Simpson, I. J., Blake, D. R., Orlando, J. J., and Barsanti, K. C.: Multi-instrument comparison and compilation of non-methane organic gas emissions from biomass burning and implications for smoke-derived secondary organic aerosol precursors, Atmos. Chem. Phys., 17, 1471–1489, 2017.

426

Hjorth, J., Lohse, C., Nielsen, C. J., Skov, H., and Restelli, G.: Products and mechanism of the gas-phase reaction between NO_3 and a series of alkenes, J. Phys. Chem., 94, 7494–7500, 1990.

429

Jenkin, M. E., Saunders, S. M., and Pilling, M. J.: The tropospheric degradation of volatile organic compounds: a protocol for mechanism development, Atmos. Environ., 31, 81–104, https://doi.org/10.1016/S1352-2310(96)00105-7, 1997 (data available at: http://mcm.york.ac.uk, last access: 12 August 2021).

433

Jenkin, M. E., Valorso, R., Aumont, B., Newland, M. J., and Rickard, A. R.: Estimation of rate coefficients for the reactions of O_3 with unsaturated organic compounds for use in automated mechanism construction, Atmos. Chem. Phys., 20, 12921–12937, https://doi.org/10.5194/acp-20-12921-2020, 2020.

437

Johnson, M. S., Strawbridge, K., Knowland, K. E., Keller, C., and Travis, M.: Long-range transport of Siberian biomass burning emissions to North America during FIREX-AQ, Atmos. Environ., 252, 118241, 2021

440

Jolly, W. M., Cochrane, M. A., Freeborn, P. H., Holden, Z. A., Brown, T. J., Williamson, G. J., and Bowman, D. M. J. S.: Climate-induced variations in global wildfire danger from 1979 to 2013, Nat. Commun., 6, 7537, 2015.

443

444 Kerdouci, J., Picquet-Varrault, B., and Doussin, J. –F.: Structure activity relationship for the gas-phase reactions of NO_3 radical
445 with organic compounds: Update and extension to aldehydes, Atmos. Environ., 84, 363-372, 2014.
446
447 Kind, I., Berndt, T., Böge, O., and Rolle, W.: Gas-phase rate constants for the reaction of NO_3 radicals with furan and methyl-
448 substituted furans, Chem. Phys. Lett., 256, 679-683, 1996.
449
450 Kodros, J., Papanastasiou, D., Paglione, M., Masiol, M. and Squizzato, S.: Rapid dark aging of biomass burning as an overlooked
451 source of oxidized organic aerosol, 117, 33028-33033, 2020.
452
453 Koss, A. R., Sekimoto, K., Gilman, J. B., Selimovic, V., Coggon, M. M., Zarzana, K. J., Yuan, B., Lerner, B. M., Brown, S. S.,
454 Jimenez, J. L., Krechmer, J., Roberts, J. M., Warneke, C., Yokelson, R. J., and de Gouw, J.: Non-methane organic gas emissions
455 from biomass burning: identification, quantification, and emission factors from PTR-ToF during the FIREX 2016 laboratory
456 experiment, Atmos. Chem. Phys., 18, 3299–3319, https://doi.org/10.5194/acp-18-3299-2018, 2018.
457
458 Krikken, F., Lehner, F., Haustein, K., Drobyshev, I., and van Oldenborgh, G. J.: Attribution of the role of climate change in the
459 forest fires in Sweden 2018, Nat. Hazards Earth Syst. Sci., 21, 2169–2179, https://doi.org/10.5194/nhess-21-2169-2021, 2021.
460
461 Kurtén, T., Møller, K. H., Nguyen, T. B., Schwantes, R. H., Misztal, P. K., Su, L., Wennberg, P. O., Fry J. L., and Kjaergaard,
462 H. G.: Alkoxy Radical Bond Scissions Explain the Anomalously Low Secondary Organic Aerosol and Organonitrate Yields
463 From alpha-Pinene + NO_3, J. Phys. Chem. Lett., 8, 2826–2834, 2017.
464
465 Kwok, E. S. C., and Atkinson, R.: Estimation of hydroxyl radical reaction rate constants for gas-phase organic compounds using
466 a structure-reactivity relationship: An update, Atmos. Environ., 29, 1685-1695, 10.1016/1352-2310(95)00069-b, 1995.
467
468 Lohmander, P.: Forest fire expansion under global warming conditions: Multivariate estimation, function properties, and
469 predictions for 29 countries, Central Asian Journal of Environmental Science and Technology Innovation, 5, 262-276, 2020.
470
471 Matsumoto, J.: Kinetics of the reactions of ozone with 2,5-dimethylfuran and its atmospheric implications, Chem. Lett., 40, 582-
472 583, 2011.
473
474 McGillen, M. R., Archibald, A. T., Carey, T., Leather, K. E., Shallcross, D. E., Wenger, J. C., and Percival, C. J.: Structure-
475 activity relationship (SAR) for the prediction of gas-phase ozonolysis rate coefficients: an extension towards heteroatomic
476 unsaturated species, Phys. Chem. Chem. Phys., 13, 2842-2849, 2011.
477
478 McGillen, M. R., Carter, W. P. L., Mellouki, A., Orlando, J. J., Picquet-Varrault, B., and Wallington, T. J.: Database for the
479 kinetics of the gas-phase atmospheric reactions of organic compounds, Earth Syst. Sci. Data, 12, 1203–1216,
480 https://doi.org/10.5194/essd-12-1203-2020, 2020.
481
482 Newland, M. J., Rea, G. J., Thüner, L. P., Henderson, A. P., Golding, B. T., Rickard, A. R., Barnes, I., and Wenger, J.:
483 Photochemistry of 2-butenedial and 4-oxo-2-pentenal under atmospheric boundary layer conditions, Phys. Chem. Chem. Phys.,
484 21, 1160-1171, 2019.
485
486 Novelli, A., Cho, C., Fuchs, H., Hofzumahaus, A., Rohrer, F., Tillmann, R., Kiendler-Scharr, A., Wahner, A., and Vereecken,
487 L.: Experimental and theoretical study on the impact of a nitrate group on the chemistry of alkoxy radicals, 23, 5474-5495, 2021.
488
489 Parrish, D. D., Lamarque, J. F., Naik, V., Horowitz, L., Shindell, D. T., Staehelin, J., Derwent, R., Cooper, O. R., Tanimoto, H.,
490 Volz-Thomas, A., Gilge, S., Scheel, H. E., Steinbacher, M. and Fröhlich, M.: Long-term changes in lower tropospheric baseline
491 ozone concentrations: Comparing chemistry-climate models and observations at northern midlatitudes, J. Geophys. Res., 119,
492 5719–5736, doi:10.1002/2013JD021435, 2014.
493

494 Ródenas, M: software for analysis of Infrared spectra. EUROCHAMP-2020 project, 2018. Available at
495 https://data.eurochamp.org/anasoft
496
497 Roman-Leshkov, Y., Barrett, C. J., Liu, Z. Y., and Dumesic, J. A.: Production of Dimethylfuran for Liquid Fuels from Biomass-
498 derived Carbohydrates, Nature, 447, 982−985, 2007.
499
500 Smith, D. F., McIver, C. D., and Kleindienst, T. E.: Primary product distribution from the reaction of hydroxyl radicals with
501 toluene at ppb NOx mixing ratios, J. Atmos. Chem., 30, 209–228, 1998.
502
503 Smith, D. F., Kleindienst, T. E., and McIver, C. D.: Primary Product Distributions from the Reaction of OH with m-, p-Xylene,
504 1,2,4- and 1,3,5-Trimethylbenzene, J. Atmos. Chem., 34, 339–364, 1999.
505
506 Sommariva, R., Cox, S., Martin, C., Borońska, K., Young, J., Jimack, P. K., Pilling, M. J., Matthaios, V. N., Nelson, B. S.,
507 Newland, M. J., Panagi, M., Bloss, W. J., Monks, P. S., and Rickard, A. R.: AtChem (version 1), an open-source box model for
508 the Master Chemical Mechanism, Geosci. Model Dev., 13, 169–183, https://doi.org/10.5194/gmd-13-169-2020, 2020.
509
510 Stewart, G. J., Acton, W. J. F., Nelson, B. S., Vaughan, A. R., Hopkins, J. R., Arya, R., Mondal, A., Jangirh, R., Ahlawat, S.,
511 Yadav, L., Sharma, S. K., Dunmore, R. E., Yunus, S. S. M., Hewitt, C. N., Nemitz, E., Mullinger, N., Gadi, R., Sahu, L. K.,
512 Tripathi, N., Rickard, A. R., Lee, J. D., Mandal, T. K., and Hamilton, J. F.: Emissions of non-methane volatile organic compounds
513 from combustion of domestic fuels in Delhi, India, Atmos. Chem. Phys., 21, 2383–2406, https://doi.org/10.5194/acp-21-2383-
514 2021, 2021a.
515
516 Stewart, G. J., Nelson, B. S., Acton, W. J. F., Vaughan, A. R., Hopkins, J. R., Yunus, S. S. M., Hewitt, C. N., Nemitz, E.,
517 Mullinger, N., Gadi, R., Rickard, A. R., Lee, J. D., Mandal, T. K., and Hamilton, J. F.: Comprehensive organic emission profiles,
518 secondary organic aerosol production potential, and OH reactivity of domestic fuel combustion in Delhi, India, Environ. Sci.:
519 Atmos., https://doi.org/10.1039/D0EA00009D, online first, 2021b.
520
521 Stone, D., Whalley, L., and Heard, D.: Tropospheric OH and HO_2 radicals: field measurements and model comparisons, Chem.
522 Soc. Rev., 41, 6348-6404, 2012.
523
524 Wang, J. J., Liu, X. H., Hu, B. C., Lu, G. Z., Wang, Y. Q.: Efficient Catalytic Conversion of Lignocellulosic Biomass into
525 Renewable Liquid Biofuels via Furan Derivatives. RSC Adv., 4, 31101− 31107, 2014.
526
527 Whelan, C. A., Eble, J. Mir, Z. S., Blitz, M. A., Seakins, P. W., Olzmann, M., and Stone D.: Kinetics of the Reactions of Hydroxyl
528 Radicals with Furan and Its Alkylated Derivatives 2-Methyl Furan and 2,5-Dimethyl Furan, *J. Phys. Chem. A*, 124, 7416–7426,
529 2020.
530
531 Wyche, K. P., Monks, P. S., Ellis, A. M., Cordell, R. L., Parker, A. E., Whyte, C., Metzger, A., Dommen, J., Duplissy, J., Prevot,
532 A. S. H., Baltensperger, U., Rickard, A. R., and Wulfert, F.: Gas phase precursors to anthropogenic secondary organic aerosol:
533 detailed observations of 1,3,5-trimethylbenzene photooxidation, Atmos. Chem. Phys., 9, 635–665, https://doi.org/10.5194/acp-
534 9-635-2009, 2009.
535
536 Yuan, Y. Zhao, X., Wang, S., and Wang, L: Atmospheric Oxidation of Furan and Methyl-Substituted Furans Initiated by
537 Hydroxyl Radicals, J. Phys. Chem. A, 121, 9306-9319, 2017.